[4]J. M. Rowell and L. Kopf, Phys. Rev. 137, A907 (1965).
[5]D. J. Scalapino, J. R. Schrieffer, and J. W. Wilkins, Phys. Rev. 148, 263 (1966).
[6]W. Meissner and R. Ochsenfeld, Naturwiss. 21, 787 (1933).
[7]B. W. Maxfield (unpublished).
[8]A. L. Schawlow and G. E. Devlin, Phys. Rev. 113, 120 (1959).
[9]R. F. Gasparovic (unpublished).
[10]W. L. McLean, Proc. Phys. Soc. (London) 79, 572 (1962).
[11]D. J. Scalapino, Y. Wada, and J. C. Swihart, Bull. Am. Phys. Soc. 9, 267 (1964).
[12]Y. Wada (unpublished).
[13]See J. R. Waldram, Advan. Phys. 13, 1 (1964), and references therein.
[14]S. B. Nam, Phys. Rev. 156, 470 (1967); 156, 487 (1967).
[15]L. H. Palmer and M. Tinkham, Phys. Rev. 165, 588 (1968).
[16]A. J. Bennett, Phys. Rev. 140, A1902 (1965).
[17]G. I. Rochlin, Phys. Rev. 153, 513 (1967).
[18]R. F. Gasparovic, Ph. D. thesis, Rutgers University, 1969 (unpublished).
[19]J. R. Schrieffer, *Theory of Superconductivity* (Benjamin, New York, 1964).
[20]R. G. Chambers, Proc. Roy. Soc. (London) A215, 481 (1952).
[21]E. A. Shapoval, Zh. Eksperim. i Teor. Fiz. 47, 1007 (1964) [Soviet Phys. JETP 20, 675 (1965)].
[22]A derivation from microscopic theory of the Ginzburg-Landau equations for strong coupling superconductors has been given by N. Menyhard, Nuovo Cimento 44B, 213 (1966); see also, G. Eilenberger and V. Ambegaokar, Phys. Rev. 158, 332 (1967); E. D. Yorke and A. Bardasis, *ibid.* 159, 344 (1967), whose results are partially confirmed experimentally by Ref. 38 below.
[23]W. J. McG. Tegart, *Electrolytic and Chemical Polishing of Metals* (Pergamon, London, 1956).
[24]R. F. Gasparovic, B. N. Taylor, and R. E. Eck, Solid State Commun. 4, 59 (1966).
[25]Detailed plots of $\lambda(T)-\lambda(0)$ as functions of $y(T)$ can be obtained from one of the authors (RFG).
[26]J. M. Lock, Proc. Roy. Soc. (London) A208, 391 (1951).
[27]K. R. Lyall and J. F. Cochran, Phys. Rev. 159, 517 (1967).
[28]J. P. Turneaure, Stanford University, High Energy Physics Laboratory HEPL Report No. 507, 1967 (unpublished).
[29]H. Hahn, H. J. Halama, and E. H. Foster, J. Appl. Phys. 39, 2606 (1968).
[30]B. C. Deaton, Phys. Rev. 177, 689 (1969).
[31]T. E. Faber and A. B. Pippard, Proc. Roy. Soc. (London) A231, 336 (1955).
[32]V. Heine, P. Nozières, and J. W. Wilkins, Phil. Mag. 13, 741 (1966).
[33]See N. W. Ashcroft and W. E. Lawrence, Phys. Rev. 175, 938 (1968), and references therein.
[34]J. E. Aubrey, Phil. Mag. 5, 1001 (1960).
[35]J. R. Anderson and A. V. Gold, Phys. Rev. 139, A1459 (1965).
[36]N. W. Ashcroft, Ph. D. thesis, University of Cambridge, 1964 (unpublished).
[37]R. Stedman, L. Almquist, G. Nilsson, and G. Rannio, Phys. Rev. 163, 567 (1967).
[38]F. W. Smith and M. Cardona, Solid State Commun. 6, 37 (1968).
[39]G. Grimvall, Physik Kondensierten Materie 8, 202 (1968).
[40]B. J. C. van der Hoeven and P. H. Keesom, Phys. Rev. 137, A103 (1965).
[41]J. Bardeen and J. R. Schrieffer, in *Progress in Low-Temperature Physics*, edited by C. J. Gorter (Interscience, New York, 1961), Vol. 3.

PHYSICAL REVIEW B VOLUME 2, NUMBER 7 1 OCTOBER 1970

Type-I and Type-II Superconductivity in Wide Josephson Junctions

Klaus Schwidtal
Institute for Exploratory Research, U. S. Army Electronics Command, Fort Monmouth, New Jersey 07703
(Received 7 May 1970)

The magnetic field dependence of the maximum dc Josephson current I_{max} of wide Pb-PbO_x-Pb Josephson junctions, for which the junction length L was about 10 times the Josephson penetration depth λ_J, has been measured. The experimental data are in excellent agreement with a theoretical prediction by Owen and Scalapino, who have numerically calculated I_{max} versus H_e for a Josephson junction with $L=10\lambda_J$, and who have also shown that the Meissner region and the vortex structure are reflected in the I_{max}-versus-H_e curve in a very characteristic way. It is shown that the boundary conditions of Owen and Scalapino's model can be most conveniently fulfilled with a cross-type junction configuration, and that the PbO_x tunneling barrier layers were fairly uniform.

I. INTRODUCTION

Wide Josephson junctions, i.e., junctions whose dimension L perpendicular to an externally applied magnetic field H_e is large with respect to the Josephson penetration depth λ_J, behave like an extreme type-II superconductor; they exhibit a Meissner effect in weak magnetic fields, and vortex

penetration starts at a critical field H_{c1}. This behavior can be probed into by studying the magnetic field dependence of the maximum tunneling supercurrent I_{max}, because the Meissner region and the vortex structure are reflected in the I_{max}-versus-H_e curve in a very characteristic way.[1]

If we consider a Josephson junction as consisting of two superconductors, usually in thin-film form, separated by a thin tunneling barrier layer that is lying in the yz plane of a coordinate system, the time-independent equation for the tunneling supercurrent density is[2-4]

$$j_x = j_0 \sin\varphi(y, z) \quad . \tag{1}$$

In Josephson's phenomenological description,[2-4] the two-dimensional field $\varphi(y, z)$ is related to φ_0, the difference of the quantum phases of the gap functions on the two sides of the barrier, and to the vector potential $\vec{A}$:

$$\varphi(y, z) = \varphi_0 - (2ed/\hbar c)\, A_x(y, z), \tag{2}$$

where d is equal to twice the superconductor penetration depth (for identical superconductors) plus the tunneling barrier layer thickness. By combining Eqs. (1) and (2) with Maxwell's equation, one obtains a differential equation which determines $\varphi(y, z)$ in the absence of a voltage bias[2,5]:

$$\frac{\partial^2\varphi}{\partial y^2} + \frac{\partial^2\varphi}{\partial z^2} = \frac{1}{\lambda_J^2}\sin\varphi \ , \tag{3}$$

where λ_J is the Josephson penetration depth[2-5]

$$\lambda_J = (\hbar c^2/8\pi e d j_0)^{1/2} \ . \tag{4}$$

The problem of theoretically predicting the maximum current I_{max} that the junction can carry in a given magnetic field is thus reduced to solving the differential equation (3), and maximizing the current, subject to the boundary conditions at the edges of the junction. Since Eq. (3) is a nonlinear differential equation, no general solution can be obtained. Only for a one-dimensional case, that is, a case in which the variables can depend only upon one spatial coordinate, solutions have been described by several authors.[1,4-6] If we assume $\varphi = \varphi(z)$, then the one-dimensional case is described by the differential equation

$$\frac{d^2\varphi}{dz^2} = \left(\frac{1}{\lambda_J}\right)^2 \sin\varphi(z), \tag{5}$$

which may be solved in terms of elliptic functions,[1,4-6] and the total tunneling supercurrent in the junction is in this case

$$I = w j_0 \int_0^L \sin\varphi(z)\, dz. \tag{6}$$

Owen and Scalapino[1] have numerically calculated I_{max} versus H_e for a "one-dimensional" Josephson junction with $L = 10\lambda_J$.

The problem of experimentally testing the predicted magnetic field dependence of I_{max} is thus reduced to the problem of experimentally realizing the one-dimensional case. This can be done, e.g., by a rectangular junction in which the y dimension w is small compared to λ_J, when H_e is applied along the y axis. Under these conditions, there is no way for spatial variations to be generated in the y direction.[1]

Several authors have measured the magnetic field dependence of I_{max} for wide Josephson junctions,[7-9] or $I_{max}(H_e = 0)$ as a function of the ratio L/λ_J,[9,10] using an in-line junction geometry to realize the one-dimensional case. However, it is rather difficult to make an in-line junction which exactly satisfies all of the conditions for realizing the one-dimensional case, and that also has a uniform tunneling barrier layer. Therefore, the agreement of the experimental data with the theoretical predictions has been of a qualitative nature only.[7-10] The best experimental agreement with the theoretically predicted magnetic field dependence of I_{max} that has been reported thus far was obtained by Clarke[11] in superconductor–normal-metal–superconductor junctions, using a cross-type junction configuration.

It is the purpose of the present paper to present for the first time experimental data of I_{max} versus H_e for the Meissner region and for the vortex region, obtained with superconductor–oxide–superconductor junctions, that are in quantitative agreement with the theoretical predictions. It will be shown that the boundary conditions of Owen and Scalapino's calculation can be realized exactly, and in a reliable way with a cross-type junction configuration similar to the one employed by Clarke,[11] and that the predicted multiple values of I_{max} for a given H_e can be detected by employing an ac measurement technique.

II. ONE-DIMENSIONAL JUNCTIONS

A. Geometrical Considerations

The term one-dimensional junction is used to indicate that the field parameter φ depends only upon one spatial coordinate, $\varphi = \varphi(z)$. Two different one-dimensional junction geometries are shown in Fig. 1: an in-line junction, Fig. 1(a), and a cross-type junction, Fig. 1(b). In both cases, we assume $w < \lambda_J$ and $w \ll L$. The external magnetic field is applied along the y axis, and the current is fed into the junction as shown in the figure.

Although the junction geometries of Figs. 1(a) and 1(b) are different, the boundary conditions on Eq. (5) are the same for both configurations. These boundary conditions are obtained from the continuity of the local magnetic field across the junction

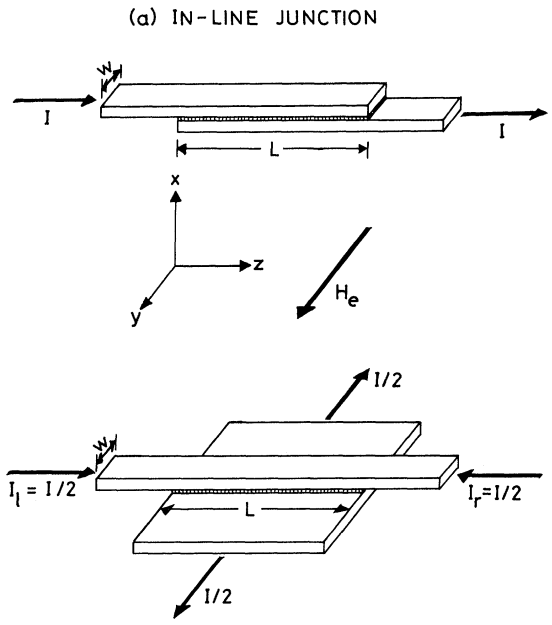

FIG. 1. Schematic drawing of two one-dimensional Josephson junction configurations: (a) in-line junction, and (b) cross-type junction. The arrows indicate the direction of the current in the thin-film strips, and the direction of the externally applied magnetic field H_e.

edges. The local magnetic field H is composed of the externally applied magnetic field H_e and the current-induced self-field H_i, $H = H_e + H_i$. H_i at $z = 0$ and $z = L$ can be obtained by applying Ampere's law to the cross section of the current-carrying film strips in the x-y plane. The current distribution in the narrow film strips is assumed to be uniform in the y direction. It is also assumed that the wide bottom film strip of the cross-type junction geometry, Fig. 1(b), may be considered as a superconducting ground plane. From the latter assumption it not only follows that the current distribution in the top film strip will indeed be uniform in the y direction, [8] but also that an image current will flow in the bottom film strip in the z direction; this image current is fed by the tunneling current. With these assumptions, we obtain for both configurations, Figs. 1(a) and 1(b),

$$H_y(z=0) = H_e - (2\pi/c)\ (I/w)\ , \tag{7a}$$

$$H_y(z=L) = H_e + (2\pi/c)\ (I/w)\ . \tag{7b}$$

Equations (7) can also be written in the form

$$H_y(L) - H_y(0) = (4\pi/c)\ (I/w)\ , \tag{8}$$

$$H_y(L) + H_y(0) = 2\ H_e\ , \tag{9}$$

which are exactly the boundary conditions used by Owen and Scalapino[1] in solving Eq. (5). Therefore, a cross-type junction configuration as shown in Fig. 1(b) may be employed in experimentally testing the theoretical predictions for the magnetic field dependence of I_{max} of one-dimensional Josephson junctions.

From the junction preparation point of view, the cross-type junction has an essential advantage over the in-line junction. For the in-line junction, both of the film strips have to be matched exactly in the y direction as well as in the z direction; this requirement does not pertain to cross-type junctions. The cross-type junction configuration has also the advantage that the left edge ($z = 0$) and the right edge ($z = L$) of the junction can be studied independently, by feeding the current into the left edge only ($I = I_l$, $I_r = 0$), or into the right edge only ($I = I_r$, $I_l = 0$). We will refer to the case in which the current is fed into one edge of the junction only as the asymmetrical case in contrast to the symmetrical case, for which $I_l = I_r = I/2$. (The current is counted as positive, when it has the direction as shown in the figure.)

B. Theoretical Considerations

The junction behaves like a type-I superconductor whenever there is a Meissner effect, that is, whenever $J_x \to 0$ and $H_y \to 0$ together within the junction. It can be shown[4] that solutions of Eq. (5) which satisfy this condition can be obtained only for local magnetic fields $H \leq H_{c1}$. The critical magnetic field H_{c1} is[2,5]

$$H_{c1} = \Phi_0/\pi\, d\lambda_J\ , \tag{10}$$

where $\Phi_0 = hc/2e$ is the quantum unit of magnetic flux.

The maximum tunneling supercurrent for the type-I region can be obtained from the condition that for this region $H = H_e + H_i \leq H_{c1}$. The current in the top film strip, and consequently H_i, is largest at the edges of the junction. Therefore, Eqs. (7) can be used to obtain for the asymmetrical case

$$I_{l,\max} = (c/4\pi)\ w\,(H_{c1} + H_e)\ , \tag{11}$$

and

$$I_{r,\max} = (c/4\pi)\, w\,(H_{c1} - H_e)\ , \tag{12}$$

and for the symmetrical case

$$I_{\max} = (c/2\pi)\ w\ (H_{c1} - |H_e|)\ . \tag{13}$$

The symmetrical case can be understood as a superposition of the two asymmetrical cases; the junction will switch to the normal conducting region, whenever the lower value of $I_{l,\max}$ or $I_{r,\max}$ is reached.

In zero externally applied magnetic field, $H_e = 0$, the maximum tunneling supercurrent is limited by the current-induced self-field H_i [5]:

$$H_e = 0 \rightarrow I_{l,\max} = I_{r,\max} = (cw/4\pi)H_{c1} = I_0(2\lambda_J/L) \quad (14)$$

for the asymmetrical case, and

$$H_e = 0 \rightarrow I_{\max} = (cw/2\pi)\,H_{c1} = I_0\,(4\lambda_J/L) \quad (15)$$

for the symmetrical case, where $I_0 = wLj_0$. I_0 is directly related to the normal tunneling resistance R_{NT} of the junction, the energy gap $\Delta(T)$ (for an identical superconductor junction), and the temperature T [12]:

$$I_0(T) = f\frac{\pi\,\Delta(T)}{2e\,R_{NT}}\tanh\left(\frac{\Delta(T)}{2kT}\right) \quad , \quad (16)$$

where the factor f is 0.788 in Pb/Pb junctions, [13,14] and is due to strong coupling effects in Pb. [13]

Once $H > H_{c1}$, the magnetic field dependence can no longer be obtained in closed form, but can be obtained only by actually solving the differential equation (5). Solutions of Eq. (5) for $H > H_{c1}$ have been described by Anderson, [4] Kulik, [6] and Owen and Scalapino. [1] These solutions describe $\varphi(z)$ as a periodic function, with the period [4,6]

$$\lambda_p = 2k\,\lambda_J\,K(k^2) \quad . \quad (17)$$

Here $K(k^2)$ is the complete elliptic integral of the first kind, and k is a parameter which has to be chosen so that the solutions are consistent with the boundary conditions. With $j_x \propto \sin\varphi$ and $H_y \propto d\varphi/dz$, j_x as well as H_y also become periodic functions with the period λ_p. This periodic pattern of $j_x(z)$ and $H_y(z)$ can be interpreted as a one-dimensional "Abrikosov array" of quantized vortices, with λ_p being the spacing of the vortices. [1,4,6]

Owen and Scalapino[1] have also numerically calculated $I_{\max}$ versus H_e for a one-dimensional junction with $L = 10\lambda_J$. This part of the theoretical analysis is of special importance from an experimental point of view, because it can be tested experimentally with available techniques. For the vortex region, Owen and Scalapino[1] predict that for a given value of H_e there may be several different current distributions with different numbers of vortices, each capable of carrying a different critical current $I_{\max}$. The experimental technique should therefore be chosen so that it allows the resolution of different values of $I_{\max}$.

III. EXPERIMENTAL RESULTS

The experimental efforts were concentrated on preparing a one-dimensional Josephson junction with $L \approx 10\lambda_J$, and studying the magnetic field dependence of $I_{\max}$. The junctions were cross-type Pb–PbO_x–Pb junctions with $L = 0.83$ mm and $w = 0.07$ mm. This geometry fulfilled the conditions $w < \lambda_J$ and $w \ll L$ for a junction with $L \approx 10\lambda_J$. The details of junction preparation and the measurement technique have been described in a previous paper. [14] The ac technique employed to display the tunneling-current–versus–voltage characteristics on an X-Y oscilloscope allowed the detection of multiple values for $I_{\max}(H_e)$, provided that the lower $I_{\max}$ value was not small with respect to the higher $I_{\max}$ value. In Fig. 2 is shown an example of an oscilloscope trace in which two different circuit load lines clearly indicate two different values of $I_{\max}$ as the intersections of the circuit load lines with the current axis. The lower circuit load line was usually weaker, or much weaker than the upper circuit load line; indicating that the probability for switching at the lower $I_{\max}$ value is small compared to the upper $I_{\max}$ value. This explains why with a dc technique, where the I-V trace is swept through only once, one gets the upper $I_{\max}$ value only.

A series of junctions was prepared, with L/λ_J ratios in the neighborhood of 10. The magnetic field dependence of $I_{\max}$ was studied while the junctions were in liquid helium under atmospheric pressure. In Fig. 3 is shown the $I_{\max}$-versus-H_e data for that junction for which the L/λ_J value came closest to 10. The general pattern of the magnetic field dependence and the degree of uniformity of the tunneling barrier layer are representative for nine junctions with L/λ_J values between 7 and 10. In those field-dependence curves, the regions of type-I behavior and type-II behavior are clearly to

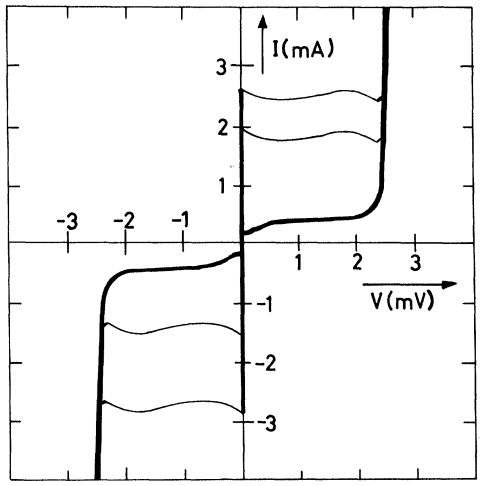

FIG. 2. I-V characteristics of a Josephson junction configuration as shown in Fig. 1(b) in an externally applied magnetic field $H_e = 0.54H_{c1}$. $I_{\max}$ is obtained from the intersection of the circuit load line with the current axis.

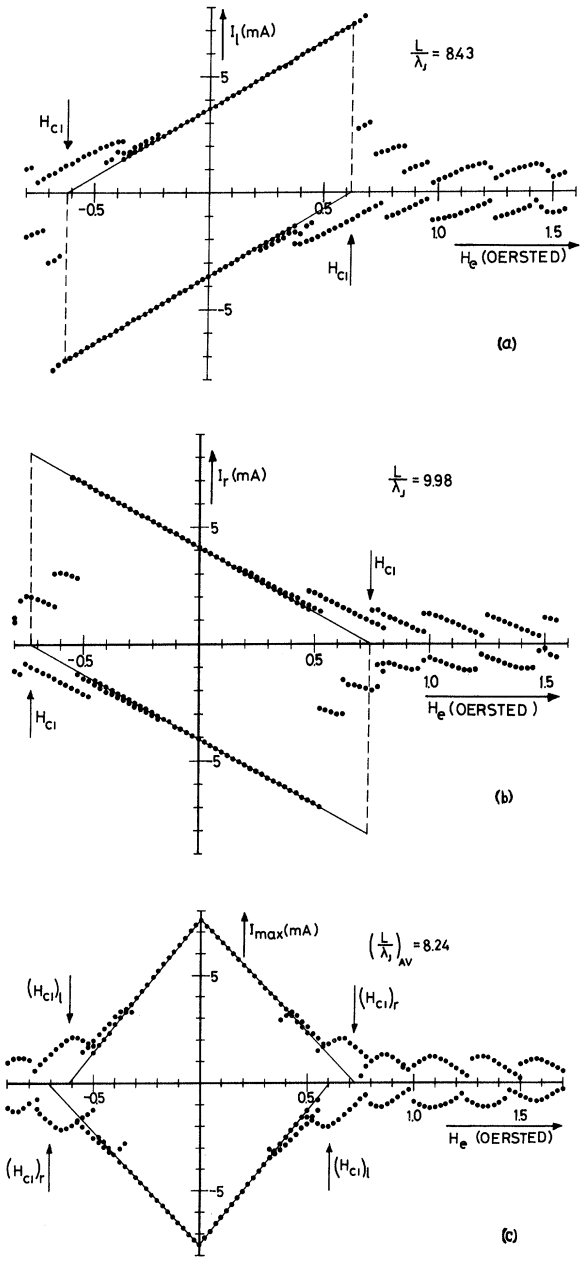

FIG. 3. Dependence of the maximum tunneling supercurrent I_{max} on the externally applied magnetic field H_e for a Josephson junction configuration as shown in Fig. 1(b). (a) Asymmetrical case, $I_{max} = I_l$, $I_r = 0$. (b) Asymmetrical case, $I_{max} = I_r$, $I_l = 0$. (c) Symmetrical case.

be seen.

A. Region of Type-I Behavior

We first consider the asymmetrical case, Figs. 3(a) and 3(b). Through the experimental points in what appears to be the Meissner region, is drawn a straight line by the least-mean-square method. These lines fit smoothly to the experimental points. From the intersection of these lines with the H_e axis, one obtains $(H_{c1})_l = 0.613$ Oe and $(H_{c1})_r = 0.725$ Oe. Within the limits of experimental error, the measured values of I_{max} ($H_e = 0$) agree with the values calculated from Eq. (14). The Meissner region is therefore correctly described by Eqs. (11) and (12) for the asymmetrical case. [In Fig. 3(a), the experimental points for the Meissner region extend beyond H_{c1}; while in Fig. 3(b) they do not extend up to H_{c1}. This is caused by the presence of the other edge, which has a higher or lower H_{c1}, respectively.]

The magnetic field dependence of I_{max} for the symmetrical case is shown in Fig. 3(c). It can easily be seen how this curve follows from a superposition of the two asymmetrical curves. For the symmetrical case, the current distribution between the left edge and the right edge of the junction was adjusted so that I_{max} had its maximum for $H_e = 0$. As can be seen from the asymmetrical case, this adjustment means for this particular junction that $I_r > I_l$. This asymmetry in the current distribution indicates that the junction was not perfectly uniform. If I_r had been made equal to I_l, as is necessarily the case for an in-line junction, the maximum of I_{max} would have been shifted from $H_e = 0$ to $H_e = [(H_{c1})_r - (H_{c1})_l]/2$. This can be easily verified from a superposition of the asymmetrical curves. Such a shift has been observed for in-line junctions by Goldman and Kreisman[7] and by Mahutte *et al.*[10]

B. Uniformity of the Barrier Layer

The difference between $(H_{c1})_l$ and $(H_{c1})_r$ indicates that the tunneling barrier layer was not perfectly uniform. A good estimate of the uniformity, or nonuniformity of the tunneling barrier layer can be obtained by comparing the L/λ_J ratios that were obtained in different ways.

(a) L/λ_J from H_{c1}. Using Eq. (10) and $d = 1090$ Å at 4.2 °K,[14] we obtain $(L/\lambda_J)_l = 8.43$ and $(L/\lambda_J)_r = 9.98$. These values are representative for the tunneling barrier layer near the left edge, and near the right edge of the junction, respectively.

(b) L/λ_J from I_{max} ($H_e = 0$), R_{NT}, and $\Delta(T)$. Using Eqs. (15) and (16) as well as $R_{NT} = 0.106\ \Omega$ and Δ (4.2 °K) = 2.53 meV, we obtain $(L/\lambda_J)_{av} = 8.24$. This value represents an average over the whole junction area, and therefore we will refer to this value as $(L/\lambda_J)_{av}$.

From the good agreement between $(L/\lambda_J)_l$ and $(L/\lambda_J)_{av}$, and the fairly good agreement between $(L/\lambda_J)_r$ and $(L/\lambda_J)_{av}$, we may conclude that the tunneling barrier layer was fairly uniform throughout the junction area.

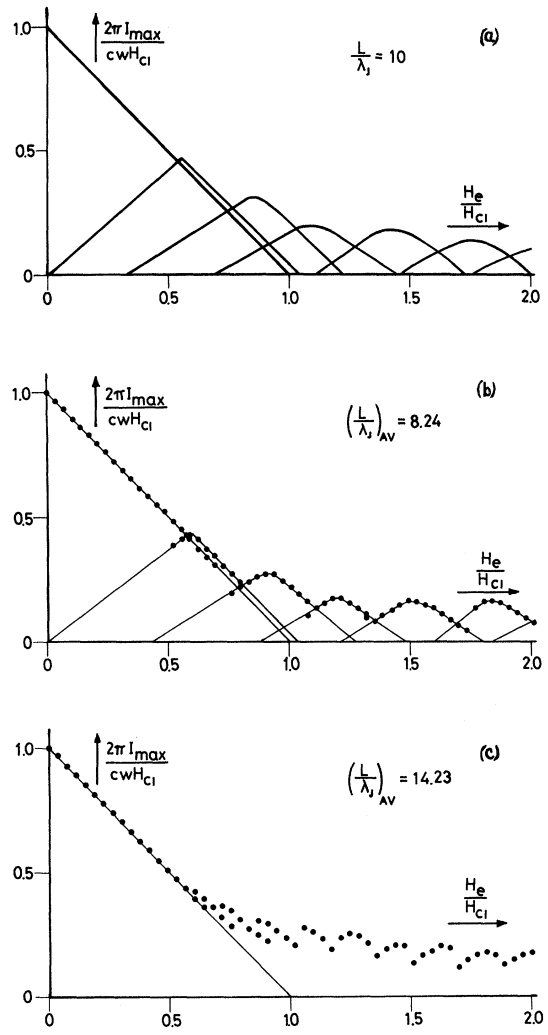

FIG. 4. Comparison of theoretically predicted and measured I_{max}-versus-H_e curves for one-dimensional Josephson junctions, normalized with respect to $H_{c1} = (2\pi/cw)\, I_{max}\,(H_e = 0)$. (a) Theoretical curve, from the data of Owen and Scalapino (Ref. 1). (b) $(+H_e, +I_{max})$ part of Fig. 3(c). (c) The measured curve for a junction with $(L/\lambda_J)_{av} = 14.23$.

C. Region of Type-II Behavior

For the region of $H > H_{c1}$ in Fig. 3, each consecutive slope for the asymmetrical case and each consecutive peak for the symmetrical case represents one more vortex in the junction. The slopes or peaks do overlap, indicating that for a given value of H_e there may exist different values for the period and shape of the vortex structure, each capable of carrying a different critical current I_{max}. This overlapping has been predicted by Owen and Scalapino.[1]

In order to quantitatively compare the magnetic field dependence of I_{max} with the theoretical prediction, Fig. 4 shows Owen and Scalapino's[1] theoretical curve, together with two experimental curves; all curves normalized with respect to H_{c1}, and in the same scale. Figure 4(b) shows the $(+H_e, +I_{max})$ part of Fig. 3(c), for which part L/λ_J, as calculated from H_{c1}, is $L/\lambda_J = 9.98$. However, it is more realistic to use the average value, $(L/\lambda_J)_{av} = 8.24$. As this average value is smaller than 10, Fig. 4(c) shows the magnetic field dependence of a junction for which $(L/\lambda_J)_{av}$ is larger than 10. By interpolating between Figs. 4(b) and 4(c), a quantitative comparison between the theoretical prediction for a junction with $L/\lambda_J = 10$, and the experimental results can still be made. We first compare Figs. 4(a) and 4(b). The agreement is quantitative, except that the spacing between the maxima of I_{max} in the vortex region is a little bit larger in the experimental figure. Comparing now with Fig. 4(c), one sees that this spacing decreases with increasing L/λ_J values. Thus by interpolating between Figs. 4(b) and 4(c) for $L/\lambda_J = 10$, a quantitative agreement between the experimental data and the theoretical curve for a junction with $L/\lambda_J = 10$ is obtained.

From a comparison of Figs. 4(b) and 4(c), one can also see that the overlapping of adjacent vortex modes increases with increasing L/λ_J values.

IV. CONCLUSIONS

The magnetic field dependence of the maximum tunneling supercurrent I_{max} for one-dimensional wide Pb–PbO_x–Pb Josephson junctions has been measured. These experimental data were compared with the theoretical prediction of Owen and Scalapino[1] for a junction with a ratio of junction length L to Josephson penetration depth λ_J of $L/\lambda_J = 10$. For a junction with $L/\lambda_J \approx 10$, for which it can be shown that the junction did fulfill the boundary conditions of Owen and Scalapino's model, and also that the tunneling barrier layer was fairly uniform, the measured I_{max}-versus-H_e curve is in excellent agreement with the theoretical prediction.

[1]C. S. Owen and D. J. Scalapino, Phys. Rev. 164, 538 (1967).

[2]B. D. Josephson, Rev. Mod. Phys. 36, 216 (1964); Advan. Phys. 14, 419 (1965).

[3]P. W. Anderson, in *Lectures on the Many-Body Problem*, edited by E. R. Caianiello (Academic, New York, 1964), Vol. 2.

[4]P. W. Anderson, in *Progress in Low Temperature Physics*, edited by C. J. Gorter (North-Holland, Amsterdam, 1967), Vol. 5.

[5]R. A. Ferrell and R. E. Prange, Phys. Rev. Letters 10, 479 (1963).

[6]I. O. Kulik, Zh. Eksperim. i Teor. Fiz. 51, 1952 (1966) [Soviet Phys. JETP 24, 1307 (1967)].
[7]A. M. Goldman and P. J. Kreisman, Phys. Rev. 164, 544 (1967).
[8]J. Matisoo, J. Appl. Phys. 40, 1813 (1969).
[9]W. Schroen and J. P. Pritchard, Jr., J. Appl. Phys. 40, 2118 (1969).
[10]C. K. Mahutte, J. D. Leslie, and H. J. T. Smith, Can. J. Phys. 47, 627 (1969).
[11]J. Clarke, Proc. Roy. Soc. (London) A308, 447 (1969).
[12]V. Ambegaokar and A. Baratoff, Phys. Rev. Letters 10, 486 (1963); 11, 104(E) (1963).
[13]T. A. Fulton and D. E. McCumber, Phys. Rev. 175, 585 (1968).
[14]K. Schwidtal and R. D. Finnegan, Phys. Rev. B 2, 148 (1970).

PHYSICAL REVIEW B VOLUME 2, NUMBER 7 1 OCTOBER 1970

Photoemission and Optical Investigation of the Electronic Structure of Ruthenium†

Kenneth A. Kress*‡ and Gerald J. Lapeyre
Department of Physics, Montana State University, Bozeman, Montana 59715
(Received 15 May 1970)

Photoemission and optical studies on vapor-deposited films and bulk samples of ruthenium are reported for the spectral range below 12.0 eV. The photoemission data locate structure in the d-like states at 0.5, 1.3, and 3.6 eV below the Fermi energy, and they show no structure due to states above the vacuum level. The data were found to be consistent with the nondirect model, with the possible exception of a small decrease in the amplitude of the structure at $E-E_F=-0.5$ eV for $h\nu>10$ eV. A combined analysis of the optical and photoemission data locates a strong peak in the d-like density of states about 1.5 eV above the Fermi energy. The studies are discussed with respect to band calculations, data for related metals, and the absence of an isotopic-mass dependence of the superconducting transition temperature. Photoemission data from a material tentatively identified as ruthenium oxide are presented.

I. INTRODUCTION

The transition metals, which contain partially filled d states, exhibit many diverse physical properties which are not found in simple metals. These properties are not easily predicted from a knowledge of the metal's atomic electron configuration as exemplified by ruthenium ($4d^7 5s^1$) which is hexagonal and nonmagnetic and by iron ($3d^7 4s^1$) which is bcc and ferromagnetic. In contrast with the $M^{-1/2}$ isotopic-mass dependence of the superconducting transition temperature found in simple metals, the transition metals exhibit many deviations.[1] The largest deviation is found in Ru which appears to have no such isotopic-mass dependence. The deviation in Ru has been treated theoretically with models that require special properties for the electronic density of states.[1,2] Few experimental studies have been reported on Ru.

We report here a study of the electronic structure of Ru using photoemission and optical data in the spectral region below 12 eV. Since, with one possible exception, the photoemission data had nondirect character over a wide range of photon energies, the photoemission data and optical studies were combined to define an optical density of initial and final states of electrons per unit energy. The optical measurements were done on vapor-deposited films of Ru. The photoemission measurements were taken from vapor-deposited films and a heat-treated bulk sample. The bulk sample provided a check for possible grain size or stress effects.

II. EXPERIMENTAL PROCEDURE

Photoemission measurements were made on vapor-deposited films of Ru under high-vacuum conditions. The films were deposited from an electron beam gun located about 0.5 m below the photocathode. The photocathode was hinged so that it could be moved into the photocollector after the vacuum deposition. Films were prepared from ingots obtained from two suppliers.[3] The photoemission data from both of these samples compared well for all films deposited below 5×10^{-8} Torr. The best pressure obtained during the deposition was $\sim1\times10^{-8}$ Torr with a base pressure of $\sim7\times10^{-10}$ Torr achieved several min after completion of the deposition.

Photoemission measurements were also performed on a sheet of bulk Ru processed by heat treating in the vacuum. A small 2×2-cm sheet was polished and degreased before spot welding onto tantalum supports. The sample was heated from behind by electron bombardment. The sheet of Ru could be heated to 1700 °C as measured by an optical pyrometer. Although the polished sheet was